

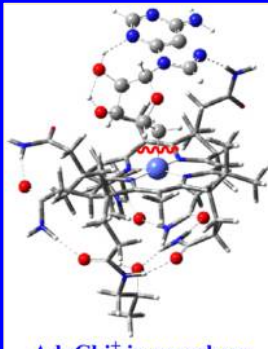
Co–C Bond Dissociation Energies in Cobalamin Derivatives and Dispersion Effects: Anomaly or Just Challenging?

Zheng-wang Qu, Andreas Hansen, and Stefan Grimme*

Mulliken Center for Theoretical Chemistry, Institut für Physikalische und Theoretische Chemie der Universität Bonn, Beringstraße 4, 53115 Bonn, North Rhine-Westphalia, Germany

Supporting Information

ABSTRACT: Accurate Co–C bond dissociation energies (BDEs) of large cobalamin derivatives in the gas phase and solution are crucial for understanding bond activation mechanisms in various enzymatic reactions. However, they are challenging for both experiment and theory as indicated by an obvious discrepancy between experimental and theoretical gas phase data for adenosylcobinamide. State-of-the-art dispersion-corrected DFT and LPNO-CCSD calculations are conducted for the Co–C BDEs of some neutral and positively charged cobalamin derivatives with adenosyl and methyl ligands and compared with available experimental gas phase and solution data to resolve the controversy. Our results from various levels of electronic structure theory are fully consistent with chemical and physical reasoning. We show undoubtedly that the Co–C bonds in complexes with the bulky adenosyl ligand are indirectly enhanced by many ligand–host non-covalent interactions and that the overall BDE are *larger* than those with the small methyl ligand in the gas phase. The additional intramolecular dispersion and hydrogen-bond interactions are significantly but not fully quenched in aqueous solution. The theoretical results including standard continuum solvation and dispersion corrections to DFT are in full accordance with experimental solution data. This is in agreement with several successful joined experimental/theoretical studies in recent years employing similar quantum chemical methodology. We see therefore no empirical basis for questioning the reliability of current dispersion corrections like D3 or VV10 to standard density functional approximations neither for these compounds nor for organometallic chemistry in general.



TPSS-D3 computed Co–C bond dissociation energies of vitamin B₁₂ derivatives:

(in kcal/mol)

| | Charged: MeCbi ⁺ | AdoCbi ⁺ |
|-----------|-----------------------------|---------------------|
| Gas-phase | 41.3 | 50.3 |
| In water | 40.4 | 29.7 |

| | Neutral: MeCbl | AdoCbl |
|-----------|----------------|--------|
| Gas-phase | 35.7 | 48.7 |
| In water | 33.6 | 27.2 |

AdoCbi⁺ in gas-phase

1. INTRODUCTION

Cobalamin (Vitamin B₁₂, Figure 1) derivatives participate in a variety of physiological enzymatic pathways that are essential to life, including blood formation, neurological function, and DNA

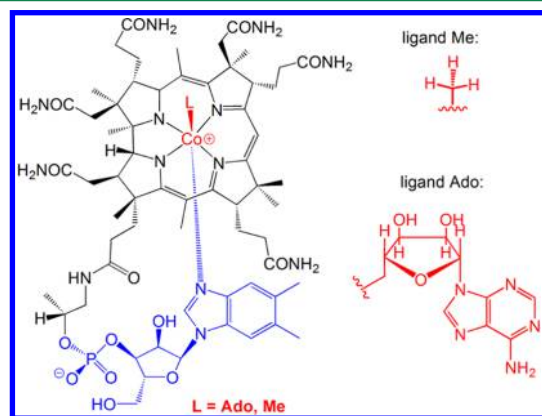


Figure 1. Molecular structures of the AdoCbl (L = Ado) and MeCbl (L = Me) complexes. The corresponding positively charged AdoCbi⁺ and MeCbi⁺ complexes are obtained by replacing the negatively charged nucleotide (blue part of the structure) by a neutral OH group.

synthesis.^{1,2} The homolysis of the extraordinary Co–C σ bond can lead to reactive radical intermediates, which play a central role in many of their biological activities as radical reservoir. In particular, methylcobalamin (MeCbl) is the cofactor in a class of enzymes that catalyze intermolecular methyl (Me) transfer reactions,³ while the adenosylcobalamin (AdoCbl) catalyzes rearrangement reactions that are mediated by radical intermediates.⁴ Impressively, the rate of homolysis of the Co–C bond in AdoCbl can be enhanced by about 12 orders of magnitude through AdoCbl-dependent enzymes relative to the uncatalyzed reaction in aqueous solution.⁵ Fundamental insights into the Co–C bond dissociation energies (BDEs, defined as dissociation energy plus zero-point vibrational energy) in different media are thus crucial for understanding the bond activation mechanism.

Experimentally, various Co–C BDEs in solution have been determined for both positively charged complexes, methylcobinamide (MeCbi⁺)⁶ and adenosylcobinamide (AdoCbi⁺),⁷ and for the neutral MeCbl^{6,8} and AdoCbl,^{5,9–12} respectively, in polar ethylene glycol and water solvents. Though reliable crystal structures of MeCbl (183 atoms) and AdoCbl (209 atoms) complexes^{13–16}

Received: January 5, 2015

Published: February 17, 2015

are available from water, the structures of the MeCbi^+ (144 atoms) and AdoCbi^+ (170 atoms) complexes in solution have been only inferred from NMR-restrained molecular constraint and MD simulations.^{17–19} No experimental structural data in the gas phase are available for these cobalamin derivatives.

Very recently, the Co–C BDEs for both complexes, AdoCbi^+ and MeCbi^+ , in the gas phase have been deduced from data-fitting of threshold collision-induced dissociation (T-CID) experiments. The respective values of 41.5 ± 1.6 and 44.6 ± 0.8 kcal mol^{−1} were used as reference to benchmark DFT methods.²⁰ Interestingly, the theoretical values as obtained from dispersion corrected density functionals (DFT-D3^{21,22}) were not only quantitatively in disagreement with the experimental values but also qualitatively worse compared to uncorrected, dispersion devoid density functionals.²⁰ While at the DFT-D3 level the larger AdoCbi^+ derivative has the *larger* BDE compared to MeCbi^+ (computed at about 53–57 kcal mol^{−1} in ref 20), the opposite is found in the T-CID measurements. Already at this point it should be mentioned that this striking disagreement between theory and experiment is difficult to understand theoretically: under the reasonable assumption that the intrinsic (local) Co–C bond energies in the AdoCbi^+ and MeCbi^+ complexes are similar, the remaining difference is due to the amount of intramolecular noncovalent interactions of a methyl compared to an adenosyl ligand with the large Cbi^+ core. Because of the additional hydrogen bonding capabilities of adenosyl and its sheer size enhancing dispersion interactions (estimated to 10–18 kcal mol^{−1} in ref 20), this should increase the AdoCbi^+ BDE relative to that of MeCbi^+ contradicting to what was measured. Notably, the Minnesota type functionals M06-L, M06, and M06-2X which account at least for the medium-range noncovalent interactions to the BDE, qualitatively agree with the DFT-D3 results.²⁰ The authors of ref 20 concluded in their study that “... even after extensive screening of numerous DFT methods, none of the presently tested dispersion corrected functionals could provide satisfactory agreement [with the T-CID derived experimental BDEs] for both MeCbi^+ and AdoCbi^+ .” The same conclusion (that current dispersion corrections like D3 are partially inadequate for organometallic systems) has very recently been drawn by the same group with the same experimental technique for two metal–ligand dissociations in a transition-metal complex benchmark.²³ It will be shown here that this conclusion has no theoretical basis and that all reliable electronic structure methods (i.e., those which try to model all interactions including dispersion accurately) show good mutual agreement for the cobalamin derivatives. Instead, on the basis of our data which also involve comparisons with condensed phase experiments, we suggest a revision of the experimental data analysis in particular for the AdoCbi^+ case. For recent successful DFT-D3 studies on transition-metal containing systems see refs 24–35.

Due to the large size and structural complexity of cobalamin derivatives, the accurate calculation of Co–C BDEs is still challenging for state-of-the-art DFT and wave function based methods,^{20,26,32,35–42} with the results being strongly dependent on the (dispersion-uncorrected) DFT functional and basis set, respectively. Early DFT calculations for Co–C BDEs were carried out mainly based on some drastically simplified model systems in the gas phase,^{36–40} while large intramolecular dispersion interactions^{20,26,31,32,35,41} as well as strong solvation effects in water^{20,35} were demonstrated more recently.

In the gas phase, the BDEs of small charged ion species were extracted from T-CID data by fitting^{43,44} to basically RRKM

models^{45,46} for the ion–molecule collision and dissociation dynamics of thermalized ions upon single-collision with inert gas. However, despite its success for small ions (mostly with less than 50 atoms),^{43–46} this analysis procedure has not been validated for large transition-metal complexes with more than 100 atoms as studied here. It is thus highly desirable to accurately compute Co–C BDEs in the gas phase and in solution, based on the full-size complex structures as well as a balanced treatment²⁶ of dispersion interactions and solvation effects.

In this work, state-of-the-art dispersion-corrected^{21,22,47,48} DFT methods^{48–53} together with accurate LPNO-CCSD⁵⁴ benchmark calculations and a COSMO-RS treatment of solvent effects^{55,56} are applied to the neutral AdoCbl and MeCbl , and the singly charged AdoCbi^+ and MeCbi^+ complexes (see Figure 1), in order to resolve the serious discrepancy between experiment and theory and to gain further insight about the important structural factors for Co–C bond energies.

2. COMPUTATIONAL METHODOLOGY

Most DFT calculations are performed with the TURBOMOLE 6.4 suite of programs using the default m4 integration grid.^{57,58} At first, all structures were fully optimized at the TPSS-D3/def2-SV(P) + COSMO(water) level of theory, which combines our default functional (TPSS meta-GGA⁵¹) with the BJ-damped²² DFT-D3 dispersion correction,²¹ the def2-SV(P) basis set,^{59,60} and the COSMO continuum solvation model⁶¹ for water (dielectric constant $\epsilon = 78.4$, refractive constant $n = 1.333$, $R_{\text{solv}} = 1.93$ Å). The density-fitting RI-J approach^{62,63} is used to accelerate the geometry optimization and numerical harmonic frequency calculations. The BP86/6-31G(d,p) optimized structures of MeCbi^+ and AdoCbi^+ as well as their radical fragments of Ado , Me , and Cbi^+ from the recent study of Chen et al.²⁰ were taken as a starting point for a more extensive conformational search of the large Cbi^+ , MeCbi^+ , and AdoCbi^+ complexes for which no crystal structure is available. To get an also consistent conformer set for the neutral Cbl , MeCbl , and AdoCbl complexes, the MeCbl crystal structure¹³ was first fully optimized, with the Me ligand being either removed or replaced by the optimized Ado group to provide initial structures for the respective Cbl and AdoCbl complexes. The optimized structures are characterized by frequency analysis to confirm the nature of located stationary points as true minima with no imaginary frequencies and to provide thermal corrections according to the modified ideal gas–rigid rotor–harmonic oscillator model.⁶⁴ All open-shell radical species (including Ado , Me , Cbi^+ , and Cbl) were treated spin-unrestricted in our DFT calculations: The resulting $\langle S^2 \rangle$ values are typically between 0.75 and 0.76 which is very close to the expected value of 0.75.

In order to get better gas phase geometries, the structures of Ado , Me , Cbi^+ , MeCbi^+ , and AdoCbi^+ are further refined at the TPSS-D3 level using the larger def2-TZVP basis set.^{65–67} The structures of Ado , Me , Cbl , MeCbl , and AdoCbl in solution are refined at the TPSS-D3/def2-TZVP + COSMO(water) level, with the COSMO solvation model being applied to maintain most crystal structure features¹⁴ of these neutral but ion-pair-like complexes. For the largest AdoCbi^+ and AdoCbl complexes, the def2-TZVP basis set leads to 3184 and 3999 contracted basis functions, respectively. The refined structures are used further to compute gas phase single-point energies and solvation energies in water. The effect of not using method specifically optimized structures in the BDE computations was found to be within 1–2 kcal mol^{−1} in test calculations. The solvation enthalpies and solvation Gibbs free energies are computed using the

COSMO-RS solvation model^{55,56} as implemented in the COSMOtherm⁶⁸ program package. The solvation enthalpies were obtained from the temperature dependence of the solvation free energies in the range of 10–60 °C, with only small differences of about 0.5 kcal mol⁻¹ between two different interpolation schemes. To check the effect of the chosen DFT functional on the gas phase energies, single-point calculations are performed using the GGA BP86-D3,^{49,69,70} meta-GGA TPSS-D3, hybrid B3LYP-D3,^{49,50} and meta-hybrid PW6B95-D3⁵² functionals together with the large def2-QZVP basis set.⁶⁷ For the largest AdoCbi⁺ and AdoCbl complexes, this leads to 7449 and 9253 contracted basis functions, respectively. For the neutral Cbl, MeCbl, and AdoCbl complexes which involve an additional nucleotide ligand with 39 atoms, the B3LYP-D3 and PW6B95-D3 single-point calculations are computationally too demanding using the large def2-QZVP basis set,^{67,71} and thus only the TPSS-D3 single-point energies are obtained for these very large complexes. As an alternative approach to properly treat dispersion interactions, TPSS-NL and B3LYP-NL single-point calculations including the electron-density-based nonlocal dispersion correction of Vydrov and van Voorhis called VV10 or DFT-NL^{47,48} are conducted for comparison with the DFT-D3 results. Furthermore, single-point calculations using the meta-hybrid M06⁵³ augmented by very-long ranged dispersion treatment (M06-D3(0), the “0” indicating the zero-damping scheme in D3) are also performed using a large integration grid (grid7) with the ORCA 3.0.1 suite of programs^{72,73} for comparison.

To further assess the performance of single-reference wave function-based methods on the gas phase energies, RI-MP2 calculations are performed using the frozen core and RI approximations as implemented in TURBOMOLE 6.4 using the TZVP⁷⁴ and QZVP⁷¹ basis sets and the corresponding TZV/C and QZV/C auxiliary basis sets.⁶⁶ Extrapolation to the MP2 complete basis set limit (CBS) is done using Helgaker's two-point extrapolation scheme separately for HF-SCF energies⁷⁵ and MP2 correlation energies.⁷⁶ More accurate and reliable LPNO-CCSD calculations⁵⁴ based on quasi-restricted orbitals⁷⁷ obtained from an unrestricted TPSS reference determinant are conducted with the TZVP basis set using the frozen core approximation and default threshold values as implemented in the ORCA 3.0.1 suite of programs.^{72,73} This is one of the largest coupled cluster and MP2 calculations on open-shell molecules ever done. An additive scheme^{78–80} was applied to estimate the CBS limit of the final LPNO-CCSD single-point energies:

$$E(\text{LPNO-CCSD}/\delta\text{CBS}) = E(\text{LPNO-CCSD}/\text{TZVP}) + [E(\text{MP2}/\text{CBS}) - E(\text{MP2}/\text{TZVP})] \quad (1)$$

The final BDEs in the gas phase are determined from the gas phase single-point energies plus the TPSS-D3/def2-SV(P) thermal corrections (in kcal mol⁻¹, at 0 or 298 K temperature and 1 atm pressure), while the BDEs in aqueous solution further include the COSMO-RS solvation enthalpies.

3. RESULTS AND DISCUSSION

3.1. Structures. It is computationally challenging to predict the global minimum gas phase structures of the MeCbi⁺ and AdoCbi⁺ complexes with many flexible amide side-chains and their intramolecular noncovalent interactions. Extensive conformational searches must be performed to find the lowest conformers of Cbi⁺ radical and MeCbi⁺ and AdoCbi⁺ before reliable BDEs can be evaluated. Based on chemical structure

considerations, two types of strong intramolecular interactions can be potentially important in determining stable conformers: the Co···O coordination bond between the terminal OH group of the very long side-chain and central Co ion; the intramolecular H-bond network (HBN) involving flexible side-chains and ligands around the relatively rigid central corrin ring. Therefore, three strategies were used to simplify the search process: First, the BP86/6-31G(d,p) optimized structures of Cbi⁺, MeCbi⁺, and AdoCbi⁺ from the recent study of Chen et al.²⁰ were taken as a starting point for our improved TPSS-D3/def2-TZVP reoptimization (labeled conformer set **A** in the following); Second, for one Co···O bond a geometry constraint is applied while the remaining HBN is adjusted and optimized *consistently* (i.e., nearly the same for each molecule in the dissociation reaction), followed by full geometry optimization without constraint (conformer set **B**); Third, the HBN is adjusted manually and then optimized to form as many as possible H-bonds without any constraint to keep a Co···O bond (conformer set **C**).

The structures of Cbi⁺, MeCbi⁺, and AdoCbi⁺ from the conformer set **C** turn out to be the spatially most compact and also most stable ones in the gas phase. The Cbi⁺ host part of the best conformer set **C** always shows six H-bonds between amide side-chains that are folded back to the central corrin ring. Interestingly, a more compact but near-degenerate conformer of Cbi⁺ (labeled as Cbi⁺′, see the SI) is also found with seven intramolecular H-bonds (two on the top side), which is only 1 kcal mol⁻¹ higher in total energy. The Cbi⁺ host part of the conformer set **B** consistently shows *five* H-bonds between amide side-chains instead; a tight Co···O coordinate bond is found only on the bottom side of Cbi⁺, but it is no longer stable when a Me or Ado ligand is added to the Co-center from the top side, suggesting the weakness of Co···O coordination. In contrast, the Cbi⁺ host part of the original set **A** from ref 20 consistently shows only *four* H-bonds between amide side-chains that are further apart from the central corrin ring. At the TPSS-D3/def2-TZVP level, the best gas phase Cbi⁺, MeCbi⁺, and AdoCbi⁺ structures from set **C** are 17.7, 9.7, and 11.2 kcal mol⁻¹ lower in total energy than those from set **B** and 28.3, 29.1, and 29.0 kcal mol⁻¹ lower than those from set **A**, respectively. These results strongly suggest that compact structures with well-organized HBN are preferred in the gas phase, which is quite different from the situation in aqueous solution.^{17–19} Although the choice of a *consistent* conformer set (i.e., from set **A**, **B**, or **C**) has only a moderate effect on the computed Co–C BDEs (changes of about 1 kcal mol⁻¹ at the TPSS-D3 level), we strongly suggest to use the minimum energy structures found in this work in future benchmark studies. Furthermore, thermal corrections are expected to be more accurate due to the quenching of some low-frequency vibrational modes in more compact structures (set **C**) compared to the original ones (set **A**).

In order to get a consistent conformer set also for the neutral Cbl, MeCbl, and AdoCbl complexes, the MeCbl crystal structure¹³ was first fully optimized at the TPSS-D3/def2-TZVP + COSMO(water) level. The Me ligand is then either removed or replaced by the optimized Ado gas phase structure to provide initial structures for the Cbl and AdoCbl complexes. After further geometry optimization, three H-bonds are consistently found on the Cbl bottom side of each complex. An additional N–H···N type H-bond is found between the added Ado ligand and one amide side-chain on the Cbl top side.

Figure 2 compares the gas phase structures of the charged Cbi⁺, MeCbi⁺, and AdoCbi⁺ and neutral Cbl, MeCbl, and AdoCbl complexes. It can be seen that the HBN on the Cbi⁺ or

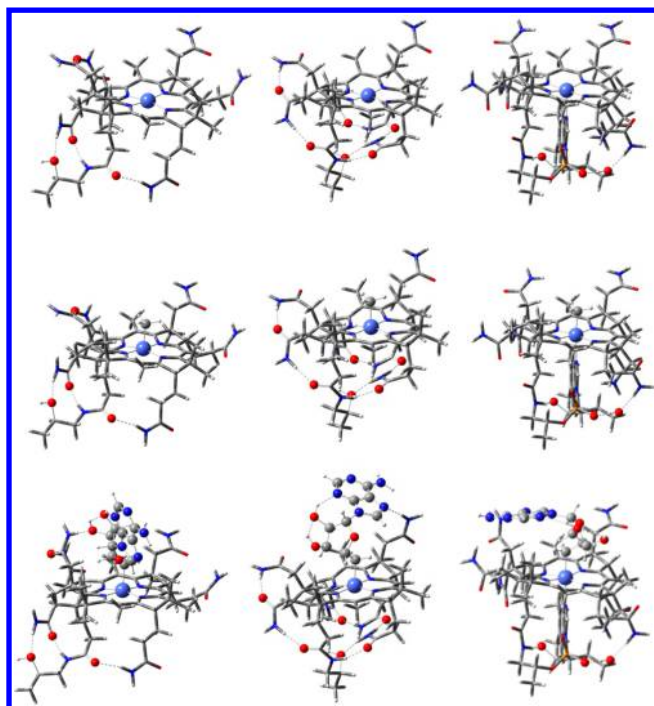


Figure 2. TPSS-D3 optimized structures (side view) of the charged Cbi^+ , MeCbi^+ , and AdoCbi^+ complexes (left: set A; middle: set C) and neutral Cbl , MeCbl , and AdoCbl complexes (right). The central Co and the H-bonded O atoms are highlighted as blue and red balls, while other C, N, and H atoms are indicated by tubes in gray, blue, and white, respectively. The Me and Ado ligands are indicated by a ball-and-stick model, while H-bonds are shown as a dashed line.

Cbl bottom side is not significantly affected by the addition of a Me or Ado ligand to the Co center, although the $\text{N}-\text{H}\cdots\text{N}$ type H-bond to the Ado ligand on the top side may enhance the BDE of Ado typically by about 3 kcal mol^{-1} in the gas phase. The $\text{N}-\text{H}\cdots\text{O}$ type H-bond to the Ado ligand instead is also possible but about 1 kcal mol^{-1} weaker. Note that in both, the crystal and solution structures of AdoCbl ,^{15,19} almost all intramolecular H-bonds are expected to be replaced by intermolecular ones with water molecules. It is thus much more difficult to predict accurate solution structures due to a generally increased conformational flexibility and strong H-bond interactions with the solvent thus requiring expensive *ab initio* molecular dynamics simulations

with explicit solvent molecules.⁸¹ Even though, our TPSS-D3 computed Co–C bond lengths of 1.976 and 1.996 Å in neutral MeCbl and AdoCbl , respectively, are reasonably close (within 0.02 Å) to the X-ray bond lengths (1.990 and 2.019 Å),¹⁴ the Co–C bond lengths of 1.957 and 1.976 Å in the charged MeCbi^+ and AdoCbi^+ complexes are computed to be slightly shorter by 0.02 Å than those in neutral MeCbl and AdoCbl , respectively, suggesting that all these single Co–C σ -bonds are electronically similar.

To estimate the effects of solvation on the Co–C BDE, we have used our consistently optimized structures (set C) and accounted for these effects by the COSMO-RS model⁶⁴ in single point energy calculations, noting the very small effects of ligand addition on the conformation of remote parts of the Co-complexes further away from the binding site. For the more open Cbi^+ , MeCbi^+ , and AdoCbi^+ structures from set A, the COSMO-RS solvation enthalpies (free energies in parentheses) are consistently more negative by 21.9, 21.4, and 26.3 (14.5, 14.2, and 16.8) kcal mol^{-1} , which hardly affects the Co–C BDE for the small Me ligand but effectively enhances that of the large Ado ligand in water by about 5 kcal mol^{-1} . On the other hand, for the more compact conformer Cbi^{++} , the solvation enthalpy is slightly less negative by 4.3 (1.5) kcal mol^{-1} .

3.2. Co–C BDEs: Effects of Alkyl Substitution. In the considered reactions one primary alkyl radical and one Co(II) -centered radical are formed after the homolytic Co–C cleavage of the cationic, closed-shell Co(III) complexes (which are the main topic of this paper). The electronic effect on the computed BDE values by changing the alkyl group can be deduced from the C–C bond cleavage in the MeMe (ethane) and AdoMe model compounds, respectively. The computed C–C and Co–C BDEs are given in the Tables 1, 2 (Cbi^+ host), and 3 (Cbl host), respectively, while various energy corrections corresponding to different measurement conditions are summarized in Table 4. As can be seen from Tables 1–3, the smaller def2-TZVP basis set seems to be already sufficient for computing reasonably converged BDEs at a DFT level which are within $0.3 \text{ kcal mol}^{-1}$ of the def2-QZVP values that are finally used. This gives confidence that our conclusions are not influenced by basis set incompleteness effects.

With the large def2-QZVP basis set, the absolute C–C BDEs increase continuously with an increasing level of sophistication in the DFT functionals, i.e., from the meta-GGA TPSS-D3, to the hybrid B3LYP-D3, and to the meta-hybrid M06-D3(0) and

Table 1. BDEs (in kcal mol^{-1}) of the L–Me Complex with the Ligand L = Me and Ado

| | BDE | | | | | | | | |
|--------------------------|------------------|------------------|------------|--------------------|------------------|------------|-----------------|------------------|------------|
| | gas, uncorrected | | | gas, ZPE-corrected | | | water | | |
| | Me ^c | Ado ^c | difference | Me ^c | Ado ^c | difference | Me ^c | Ado ^c | difference |
| BP86-D3 | 94.8 | 93.0 | 1.8 | 85.4 | 84.6 | 0.7 | 86.8 | 85.2 | 1.5 |
| TPSS-D3 ^a | 91.9 | 90.1 | 1.8 | 82.5 | 81.8 | 0.8 | 83.9 | 82.4 | 1.5 |
| TPSS-D3 | 91.7 | 89.9 | 1.8 | 82.2 | 81.5 | 0.7 | 83.7 | 82.2 | 1.5 |
| TPSS-NL | 93.3 | 91.9 | 1.4 | 83.8 | 83.5 | 0.3 | 85.3 | 84.1 | 1.1 |
| B3LYP-D3 | 92.8 | 91.6 | 1.2 | 83.4 | 83.3 | 0.2 | 84.8 | 83.9 | 0.9 |
| B3LYP-NL | 94.2 | 93.2 | 1.0 | 84.8 | 84.9 | −0.1 | 86.2 | 85.5 | 0.7 |
| PW6B95-D3 | 97.7 | 96.1 | 1.6 | 88.3 | 87.8 | 0.5 | 89.7 | 88.4 | 1.3 |
| M06-D3(0) | 96.5 | 95.5 | 1.0 | 87.1 | 87.1 | 0.0 | 88.5 | 87.7 | 0.8 |
| CCSD/ δCBS | 97.8 | 98.7 | −0.9 | 88.4 | 90.3 | −2.0 | 89.8 | 91.0 | −1.2 |
| exptl ^b | 97.3 | | | 87.8 | | | 89.2 | | |
| | | | | (± 0.4) | | | | | |

^aCalculated with the def2-TZVP basis set. ^bBack-corrected from experimental $\Delta H_{298}^0(\text{gas}) = 90.1 \pm 0.4 \text{ kcal mol}^{-1}$ in ref 82. ^cLigand.

Table 2. BDEs (in kcal mol⁻¹) of the L–Cbi⁺ Complex with the Ligand L = Me and Ado

| | BDE | | | | | | | | |
|--|------------------|------------------|------------|--------------------|------------------|------------|-------------------|------------------|------------|
| | gas, uncorrected | | | gas, ZPE-corrected | | | water | | |
| | Me ^g | Ado ^g | difference | Me ^g | Ado ^g | difference | Me ^g | Ado ^g | difference |
| BP86-D3 | 49.6 | 60.5 | −11.0 | 45.5 | 57.2 | −11.7 | 44.6 | 36.6 | 8.0 |
| TPSS-D3 ^a | 45.9 | 55.1 | −9.1 | 41.9 | 51.7 | −9.8 | 41.0 | 31.1 | 9.9 |
| TPSS-D3 | 45.4 | 53.6 | −8.3 | 41.3 | 50.3 | −9.0 | 40.4 | 29.7 | 10.7 |
| TPSS-NL | 48.4 | 59.2 | −10.8 | 44.3 | 55.9 | −11.5 | 43.4 | 35.3 | 8.2 |
| B3LYP-D3 ^b | 35.7 | 43.8 | −8.1 | 31.6 | 40.5 | −8.8 | 30.8 | 19.9 | 10.9 |
| B3LYP-NL ^b | 37.4 | 46.6 | −9.2 | 33.3 | 43.3 | −9.9 | 32.5 | 22.7 | 9.8 |
| PW6B95-D3 ^b | 34.1 | 40.5 | −6.4 | 30.0 | 37.1 | −7.1 | 29.2 | 16.5 | 12.6 |
| M06-D3(0) | <i>c</i> | <i>c</i> | −9.9 | <i>c</i> | <i>c</i> | −10.6 | <i>c</i> | <i>c</i> | 9.1 |
| CCSD/δCBS | 32.8 | 43.0 | −10.2 | 28.7 | 39.7 | −10.9 | 27.9 | 19.1 | 8.8 |
| exptl (from sol. data) ^d | 42.0 | 58.4 | −16.5 | 37.9 | 55.1 | −17.2 | 37.0 ^e | 34.5 | 3.5 |
| | | | | | | | (±3.0) | (±1.8) | (±3.5) |
| exptl (from gas phase data) ^f | 48.7 | 44.8 | 3.8 | 44.6 | 41.5 | 3.1 | 43.7 | 20.9 | 22.8 |
| | | | | (±0.8) | (±1.6) | (±1.8) | | | |

^aCalculated with the def2-TZVP basis set. ^bDue to a convergence problem for Cbi⁺, these data are estimated using the more compact but near-degenerate conformer Cbi⁺ (see the SI) instead. ^cNot available due to a convergence problem. ^dBack-corrected from aqueous solution data in refs 5, 6, and 83, with error bars in parentheses. ^eA larger BDE value of 42(±5) for MeCbi⁺ in water is obtained by photoacoustic calorimetric data in ref 84. ^fBack-corrected from the T-CID thresholds at 0 K in ref 20. ^gLigand.

Table 3. BDEs (in kcal mol⁻¹) of the L–Cbl Complex with the Ligand L = Me and Ado

| | BDE | | | | | | | | |
|---|------------------|------------------|------------|--------------------|------------------|------------|-------------------|------------------|------------|
| | gas, uncorrected | | | gas, ZPE-corrected | | | water | | |
| | Me ^d | Ado ^d | difference | Me ^d | Ado ^d | difference | Me ^d | Ado ^d | difference |
| BP86-D3 | 43.4 | 61.3 | −17.9 | 38.5 | 55.4 | −16.9 | 36.4 | 33.8 | 2.6 |
| TPSS-D3 ^a | 41.1 | 56.1 | −15.0 | 36.2 | 50.2 | −14.0 | 34.0 | 28.6 | 5.4 |
| TPSS-D3 | 40.6 | 54.6 | −14.0 | 35.7 | 48.7 | −13.0 | 33.6 | 27.2 | 6.4 |
| TPSS-NL | 45.3 | 63.1 | −17.8 | 40.4 | 57.2 | −16.8 | 38.2 | 35.6 | 2.6 |
| B3LYP-D3 | 30.3 | 44.4 | −14.1 | 25.4 | 38.5 | −13.1 | 23.3 | 17.0 | 6.3 |
| B3LYP-NL | 33.8 | 49.4 | −15.6 | 29.0 | 43.5 | −14.6 | 26.8 | 22.0 | 4.8 |
| PW6B95-D3 | 30.5 | 44.0 | −13.5 | 25.6 | 38.1 | −12.5 | 23.5 | 16.6 | 6.9 |
| exptl (from solution data) ^b | 43.0 | 57.4 | −14.4 | 38.2 | 51.5 | −13.4 | 36.0 ^c | 30.0 | 6.0 |
| | | | | | | | (±4) | (±2) | (±4.5) |

^aCalculated with the def2-TZVP basis set. ^bBack-corrected from aqueous solution data in refs 5 and 6. ^cA larger BDE value of 39(±5) for MeCbl in water is obtained by photoacoustic calorimetric data in ref 84. ^dLigand.

Table 4. TPSS-D3 and COSMO-RS Computed Energy Corrections (in kcal mol⁻¹) to the Electronic BDEs of L–M Complexes with L = Me and Ado and M = Me, Cbi⁺, and Cbl

| | host M | | | | | | | | |
|------------------------|-----------------|------------------|------------|------------------|------------------|------------|-----------------|------------------|------------|
| | Me | | | Cbi ⁺ | | | Cbl | | |
| | Me ^b | Ado ^b | difference | Me ^b | Ado ^b | difference | Me ^b | Ado ^b | difference |
| D3 (TPSS) ^a | 1.2 | 2.4 | −1.2 | 8.2 | 23.4 | −15.2 | 9.0 | 33.6 | −24.6 |
| ZPE | −9.4 | −8.4 | −1.1 | −4.1 | −3.3 | −0.7 | −4.9 | −5.9 | 1.0 |
| H298 | −7.2 | −6.6 | −0.6 | −3.1 | −2.9 | −0.2 | −3.7 | −4.4 | 0.7 |
| G298 | −17.9 | −18.4 | 0.5 | −13.6 | −20.3 | 6.7 | −14.5 | −24.9 | 10.4 |
| H _{sol} | −0.9 | −1.2 | 0.3 | −1.8 | −21.0 | 19.2 | −3.4 | −23.1 | 19.7 |
| G _{sol} | 4.8 | 4.9 | −0.2 | 5.0 | −6.5 | 11.5 | 4.6 | −7.8 | 12.5 |

^aD3 (TPSS): dispersion correction of the TPSS functional; ZPE: zero-point energy correction; H298: enthalpy correction at 298 K; G298: free energy correction at 298 K; H_{sol}: solvation enthalpy correction in water computed with COSMO-RS; G_{sol}: solvation free energy correction in water computed with COSMO-RS. ^bLigand L.

PW6B95-D3. In contrast, the semilocal BP86-D3 functional consistently leads to about 3 kcal mol⁻¹ larger C–C BDEs than TPSS-D3. The same trend is observed for the density-dependent dispersion corrected TPSS-NL and B3LYP-NL functionals, despite that somewhat larger corrections are computed by the NL-scheme in general for such thermochemical properties⁴⁸

especially for larger systems. The deviation to the experimental gas phase value for ethane⁸² diminishes in the same series. LPNO-CCSD/δCBS calculations and the best density functional (PW6B95-D3) also agree within 2.6 kcal mol⁻¹ for both C–C BDEs. Despite the fact that the TPSS-D3 functional underestimates the absolute C–C BDEs by 6–9 kcal mol⁻¹, the relative

C–C BDE between MeMe and AdoMe is consistently computed by all DFT functionals to within 1 kcal mol^{−1}. Though a larger C–C BDE would be expected for the more electronegative Me ligand, it turns out that the relative C–C BDE between Me and Ado is very small mainly due to a compensation between a 1.2 kcal mol^{−1} stronger dispersion and a 1.1 kcal mol^{−1} smaller zero-point energy correction (Table 4) for the more bulky Ado ligand. As noted above, this difference between Me and Ado is expected to increase significantly in the “real” systems due to the larger size difference of methyl compared to the corrin rings.

3.3. Co–C BDEs: Relative versus Absolute Values. In general, it is easier to calculate *relative* rather than *absolute* BDEs, due to favorable error cancellation for the former quantity as already seen above for the simple C–C homolysis. Compared to this example, however, the open-shell 3d⁷ Co(II)-radicals formed by Co–C homolysis of the various closed-shell 3d⁶ Co(III)-complexes are expected to exhibit an electronically more complex structure than the alkyl radicals due to the presence of spatially compact, nearly degenerate 3d-manifold of states. This is known to degrade the performance of hybrid functionals with an increasing amount of Fock exchange as well as the single-reference based CCSD method. Nonetheless, the use of quasi-restricted orbitals obtained from an unrestricted TPSS determinant does not only (approximately) cure the spin-contamination problem in single-reference correlation methods but also static correlation is modeled to some extent.⁵⁴ As seen from Tables 2 and 3, in contrast to the case of the C–C bonds, the Co–C BDEs for the various closed-shell Co(III)-complexes tend to *decrease* for functionals with an increasing amount of Fock exchange as also observed in recent DFT studies.^{20,26,32} Because the relative values of the BDE for Me and Ado ligands could be more accurately computed in comparison with experiment, we discuss the methodological effect on this property first and note in passing that relative BDEs should be reasonably computable also for methods that do not yield very accurate absolute values.

As can be seen from Figure 3, the computed *relative* Co–C BDEs between the Me and Ado ligands are insensitive to the

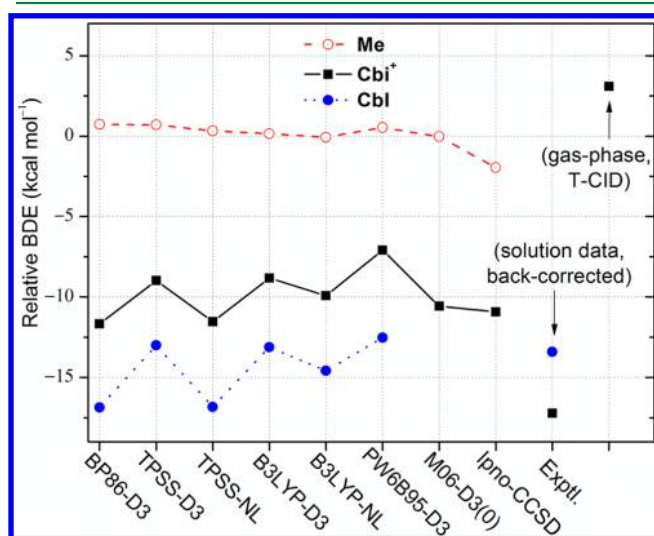


Figure 3. Relative ZPE-corrected BDEs (in kcal mol^{−1}) between Me and Ado ligands for the three different hosts Me, Cbi⁺, and Cbl with various electronic structure methods and in comparison with experimental data (referring always to the gas phase but in one case derived from solution values by back-correction with theoretical data).

DFT functional choice with small variations of up to 4 kcal mol^{−1}. This is attributed to a cancellation of errors in the open-shell Cbi⁺ and Cbl Co(II)-radicals which are the same in both bond dissociations. Nevertheless, we prefer for our following discussion a method which also provides accurate absolute BDEs. In cases with some multireference character, semilocal functionals like the meta-GGA TPSS-D3 seem to be more robust because of their implicit account of static correlation effects. Note that none of our basic conclusions are affected by the choice of the particular density functional, as the values for a wide variety of methods including density-dependent dispersion corrections as given in Tables 1–3 (also in Figure 3 for comparison) do not differ significantly from each other. They will be discussed below in comparison if appropriate. However, already at this point it should be emphasized that *all* applied quantum chemical methods including CCSD are in striking disagreement with the relative BDEs for Me and Ado from T-CID experiments. According to our results using state-of-the-art quantum chemical methods using two different dispersion corrections and various (meta, hybrid) density functionals, the BDE of the smaller Me ligand is *lower* than for the larger Ado ligand. This is in agreement with simple physicochemical considerations discussed below where also effects of dispersion and noncovalent interactions are considered in more detail (see section 3.6).

3.4. Co–C BDEs in the Gas Phase. As can be seen from Table 2 and Figure 3, the TPSS-D3 Co–C BDEs of MeCbi⁺ and AdoCbi⁺ at 0 K are 41.3 and 50.3 kcal mol^{−1}, respectively, with the former being 9.0 kcal mol^{−1} smaller. Due to more favorable dispersion and additional H-bond interactions with the Ado ligand, the larger Co–C BDEs for AdoCbi⁺ are understandable. This view is supported by calculations based on nonlocal (VV10) dispersion corrected functionals,⁴⁷ hybrid functionals as well as LPNO-CCSD calculations. For comparison, the experimental T-CID derived gas phase Co–C BDEs of MeCbi⁺ and AdoCbi⁺ are 44.6 ± 0.8 and 41.5 ± 1.6 kcal mol^{−1}, respectively, with the latter being surprisingly 3.1 ± 1.8 kcal mol^{−1} smaller²⁰ despite the fact that the former is reasonably reproduced by our TPSS-D3 calculations based on the lowest energy conformer set C. The *relative* Co–C BDE between MeCbi⁺ and AdoCbi⁺ varying between −7 and −11 kcal mol^{−1} is only weakly dependent on the electronic structure method employed as noted above. The good agreement between the D3 and NL dispersion corrected results is also encouraging and further supporting the reliability of our gas phase computed BDEs. The M06 functional which misses the very long part of the dispersion energy but includes the medium-range part yields similar results. The relative Co–C BDE between MeCbi⁺ and AdoCbi⁺ (−17.2 kcal mol^{−1}) from back-corrected solution data^{5,6,83} is even more negative than our computed value, mainly due to more open structures in aqueous solution^{17–19} that lead to a better solvation for the larger AdoCbi⁺ complex (as already seen for the conformer set A).

It is interesting to consistently compare our computed Co–C BDEs with recent computational studies based on either full-size²⁰ or simplified^{32,35} cobalamin and cobinamide systems. Based on the BP86 optimized full-size structures for the MeCbi⁺ and AdoCbi⁺ complexes,²⁰ the final ZPE-corrected Co–C BDEs at single-point BP86-D3 (47.1 and 58.6 kcal mol^{−1}) and B3LYP-D3 (29.9 and 39.3 kcal mol^{−1}) levels are very close within 2 kcal mol^{−1} to our BP86-D3 (45.5 and 57.2 kcal mol^{−1}) and B3LYP-D3 (31.6 and 41.5 kcal mol^{−1}) results based on more compact structures. However, based on the BP86 + COSMO(ϵ = 80) optimized geometries for the AdoCbl model system by replacing the negatively charged nucleotide with the smaller but neutral

histidine (imidazole) as trans-ligand,³⁵ the ZPE-uncorrected Co–C BDEs of 51.4 and 34.8 kcal mol^{−1} at the single-point BP86-D3 and B3LYP-D3 levels are about 10 kcal mol^{−1} smaller than our computed results of 61.3 and 44.4 kcal mol^{−1}, respectively. In contrast, based on the BP86 optimized geometries for the further simplified MeCbl model system by using neutral histidine as trans-ligand and removing all side-chains on the corrin-ring,³² the ZPE-corrected Co–C BDEs of 39.7 and 24.7 kcal mol^{−1} at the single-point BP86-D3 and B3LYP-D3 levels are very close to our results of 38.5 and 25.4 kcal mol^{−1}, respectively. This demonstrates the importance of using the full complexes in computational studies for a meaningful comparison with experimental data.

3.5. Co–C BDEs in Water. To further test the reliability of our calculations, the Co–C BDEs at 298 K in aqueous solution are estimated using the same gas phase energies together with the computed thermal and solvation corrections from the COSMO-RS model (Table 4). This treatment employs the optimized gas phase structures and is therefore not fully conclusive but should be sufficient at a semiquantitative level because the error spread of the experimental values is also quite large. The TPSS-D3 computed Co–C BDEs of MeCbi⁺ and AdoCbi⁺ in water are 40.4 and 29.7 kcal mol^{−1}, respectively, with the latter being more sensitive to solvation effects due to potentially strong H-bonding interactions and conformational changes. Compared with the experimental solution data (37 ± 3⁶ or 42 ± 5⁴⁸ for MeCbi⁺ and 34.5 ± 1.8⁸³ kcal mol^{−1} for AdoCbi⁺), our estimates reproduce both absolute and relative Co–C BDEs in solution quite well. Using geometrically more open solution structures might further improve the agreement. Indeed, even better results are obtained for the neutral MeCbl and AdoCbl complexes based on X-ray crystal structures (Table 3): compared with experimental solution data (36 ± 4⁶ or 39 ± 5⁴⁸ for MeCbl and 30 ± 2⁵ kcal mol^{−1} for AdoCbl), the TPSS-D3 computed absolute BDEs of 33.6 and 27.2 kcal mol^{−1} are about 3 kcal mol^{−1} too small, while the computed relative BDE of 6.4 kcal mol^{−1} agrees very well with the experimental value of 6.0 ± 4.5 kcal mol^{−1}. This good agreement between theory and experiment for the condensed phase further supports the reliability of TPSS-D3 for these systems. In turn, this and the results given above from the other quantum chemical methods seriously question the experimentally derived (T-CID) gas phase Co–C BDE of AdoCbi⁺ which seems to be underestimated by about 10 kcal mol^{−1} if reasonable error bars of our treatment are assumed.

Based on our TPSS-D3 calculations for the base-removed MeCbi⁺ and AdoCbi⁺ and the base-on MeCbl and AdoCbl complexes, it is also possible to discuss the effects of base coordination on the Co–C BDEs. Upon base coordination, the Co–C BDE of Me and Ado ligands are decreased by 5.6 and 1.6 kcal mol^{−1} in the gas phase and by 6.8 and 2.5 kcal mol^{−1} in water, respectively, suggesting a 4 kcal mol^{−1} stronger destabilizing effect of base coordination on the Co–C BDEs for the smaller Me compared to the Ado ligand.

3.6. Co–C BDEs: The Role of Dispersion, Solvation, and Entropy Effects. It should be pointed out that the D3 dispersion correction^{21,22} is crucial for the accuracy of our TPSS-D3 calculations in order to predict both absolute and relative Co–C BDEs, especially for these relatively large systems.³² Similar conclusions hold for other functionals or the NL-dispersion corrected methods. As can be seen from Table 4, the D3 contribution to the BDE is very small for the relatively small functional groups (1.2 kcal mol^{−1} for Me–Me) but

increases significantly for the larger cases (33.6 kcal mol^{−1} for Ado–Cbl). As can be seen from Figure 3, for the large Cbi⁺ and Cbl hosts, the net D3-contributions to the relative BDE of −15.2 and −24.6 kcal mol^{−1} are already sizable and decisive for the correct relative Co–C BDEs between the Me and Ado ligands of around −10 and −15 kcal mol^{−1}, respectively.

The Co–C BDEs are not very sensitive to temperature changes with only small zero-point and enthalpy corrections to the electronic BDE (within 2 kcal mol^{−1} at room temperature). In contrast, the effect of solvation in water on the Co–C BDEs is strongly dependent on the H-bonding ability of the ligands: for the large Cbi⁺ and Cbl hosts, the effect is relatively small (−1.8 and −3.4 kcal mol^{−1}) for the non-H-bonding Me but strongly destabilizing (−21.0 and −23.1 kcal mol^{−1}) for the H-bonding Ado ligand, respectively, which eventually overcompensates the 10–15 kcal mol^{−1} larger BDEs for the Ado ligand in gas phase. Moreover, it is also important to consider the destabilizing entropy effects (negative free energy corrections) to the bond dissociation free energies (BDFs) that determine the thermodynamic stability. For the large Cbi⁺ and Cbl hosts, the free energy corrections are 6.7 and 10.4 kcal mol^{−1} more negative for the Ado than for the smaller Me ligand at 298 K, which almost compensates the 10–15 kcal mol^{−1} larger BDEs for of Ado in the gas phase and may even reverse the relative thermodynamic stabilities of Co–C bonds at higher temperatures.

3.7. Co–C BDEs: Why Are Those with the Ado Ligand Experimentally Underestimated? According to our theoretical data, the experimental gas phase Co–C BDE of the Ado ligand is significantly underestimated, and we suggest that the fitting procedure⁴⁴ used to extract the dissociation threshold from the T-CID data at 343 K²⁰ might be responsible. One possible explanation is related to a “kinetic shift” problem of the CID threshold, which can be more sizable for larger complexes (or larger ligands at the same host). Accurate estimation of “kinetic shifts” for complexes from the combinations of large hosts and ligands of quite different size is crucial for obtaining reliable Co–C BDEs. At present, the state-of-the-art T-CID fitting procedure⁴⁴ has been validated only for relatively small ions using density-of-state functions fitted to small ions with up to 50 atoms, which may not be necessarily accurate for larger complexes with more than 140 atoms as in AdoCbi⁺. Using more accurate density-of-state functions based on DFT calculations on full-size complexes may help to resolve this issue. Second, the threshold energy E_0 (activation enthalpy) extracted directly from T-CID data at a single temperature may inevitably include some entropy effects that may effectively reduce the thermodynamic stability of the larger Ado ligand in gas phase. Usually, activation parameters should be determined by *variable*-temperature experiments. According to our TPSS-D3 calculations, the Co–C bond of AdoCbi⁺ becomes 1 kcal mol^{−1} less stable at a free energy level than that of MeCbi⁺ in the gas phase at 343 K.

4. CONCLUSIONS

State-of-the-art dispersion-corrected DFT methods in various flavors together with *ab initio* wave function methods were applied to compute the Co–C bond dissociation energies (BDEs) in large cobalamin and cobinamide complexes both in gas phase and in solution. The main aim was to resolve a striking discrepancy between theory and experiment and to elucidate the important role of long-range (also called London) dispersion interactions for a prototype chemical reaction of a large system. The conclusions are expected to be relevant for many organo-metallic and bioinorganic (catalytically active) systems.

From a theoretical point of view, the system is *not* challenging regarding the intramolecular noncovalent interactions and the dispersion contributions. The application of dispersion corrections to standard density functionals tends to diminish the differences between functionals of different type (including those of the Minnesota class). The most notable effect on the computed absolute Co–C BDEs is the amount of included nonlocal Fock exchange, as also reported previously for similar systems involving a 3d transition metal.^{26,31,32,35,39,41} the experimental absolute BDEs could be better reproduced by semilocal (GGA or meta-GGA) density functionals and tend to decrease with the amount of nonlocal Fock exchange in a hybrid functional. However, for the here more important relative trend in the BDE with increasing size of the dissociating ligand, we find consistent results for *all* applied electronic structure methods which take long-range correlation effects properly into account including high-level coupled-cluster treatments.³² We see therefore no empirical basis for questioning current dispersion corrections like D3 or NL(VV10) for organometallic chemistry.²³ The downsides of nonelectronic corrections like D3 for metallic systems have been discussed before,^{21,85} but the errors in the reactions considered here seem to be small in agreement with the conclusions in previous studies.^{24–35} A recent, very detailed investigation of the dispersion effect for the dissociation of a Pd–Pd bond (which has a much larger metal-dispersion contribution than the here considered Co–C case) revealed only a small overshooting of the standard D3 scheme and a very good accuracy of the NL(VV10) correction in comparison to experimental and DLPNO-CCSD(T) results.²⁹

In aqueous solution the intramolecular noncovalent interactions are overcompensated by stronger bond *destabilizing* solvation effects mostly due to H-bonding with the water solvent molecules, and hence we predict an “inversion” of the BDE trend between Me and Ado substituents when going from the gas phase into aqueous solution. This view is supported by the good agreement of theoretical (TPSS-D3 including implicit COSMO-RS solvation) and experimental values for the Me and Ado systems in water. In fact, this finding (which is based on the critical gas phase BDE) provides a strong indication that the experimental gas phase value for AdoCbi⁺ is incorrect. While the fitting procedure⁴⁴ used to extract Co–C BDEs from T-CID data based on density-of-state functions fitted to small ions seems applicable for the small Me ligand, it might lead to underestimated BDEs for the large Ado ligand. Tentatively, an inaccurate account for “kinetic shifts” and/or entropy effects in the experiments is suggested as a reason.

■ ASSOCIATED CONTENT

■ Supporting Information

TPSS-D3/def2-TZVP optimized geometries; TPSS-D3/def2-SV(P) zero-point and thermal corrections; BP86/def2-TZVP COSMO-RS solvation energies in water and D3-dispersion corrections to the TPSS functional; TPSS-D3, TPSS-NL, B3LYP-D3, B3LYP-NL, M06-D30, and PW6B95-D3 single-point energies using the large def2-QZVP basis set; MP2/TZVP, MP2/QZVP, and LPNO-CCSD/TZVP single-point energies. This material is available free of charge via the Internet at <http://pubs.acs.org>.

■ AUTHOR INFORMATION

Corresponding Author

*E-mail: grimme@thch.uni-bonn.de.

Notes

The authors declare no competing financial interest.

■ ACKNOWLEDGMENTS

We are grateful to the Deutsche Forschungsgemeinschaft within the SFB 813 “Chemistry at Spin Centers” for financial support.

■ REFERENCES

- (1) Kräutler, B.; Arigoni, D.; Golding, B. T. *Vitamin B12 and B12-proteins*; Wiley-VCH: Weinheim, 1998.
- (2) Banerjee, R. *Chemistry and Biochemistry of B12*; John Wiley & Sons: New York, 1999.
- (3) Matthews, R. G. *Acc. Chem. Res.* **2001**, *34*, 681–689.
- (4) Halpern, J. *Science* **1985**, *227*, 869–875.
- (5) Hay, B. P.; Finke, R. G. *J. Am. Chem. Soc.* **1986**, *108*, 4820–4829.
- (6) Hung, R. R.; Grabowski, J. J. *J. Am. Chem. Soc.* **1999**, *121*, 1359–1364.
- (7) Garr, C. D.; Sirovatka, J. M.; Finke, R. G. *Inorg. Chem.* **1996**, *35*, 5912–5922.
- (8) Martin, B. D.; Finke, R. G. *J. Am. Chem. Soc.* **1992**, *114*, 585–592.
- (9) Finke, R. G.; Hay, B. P. *Inorg. Chem.* **1984**, *23*, 3041–3043.
- (10) Halpern, J.; Kim, S. H.; Leung, T. W. *J. Am. Chem. Soc.* **1984**, *106*, 8317–8319.
- (11) Hay, B. P.; Finke, R. G. *Polyhedron* **1988**, *7*, 1469–1481.
- (12) Garr, C. D.; Finke, R. G. *Inorg. Chem.* **1993**, *32*, 4414–4421.
- (13) Rossi, M.; Glusker, J. P.; Randaccio, L.; Summers, M. F.; Toscano, P. J.; Marzilli, L. G. *J. Am. Chem. Soc.* **1985**, *107*, 1729–1738.
- (14) Mebs, S.; Henn, J.; Dittrich, B.; Paulmann, C.; Luger, P. *J. Phys. Chem. A* **2009**, *113*, 8366–8378.
- (15) Randaccio, L.; Geremia, S.; Nardin, G.; Wuerger, J. *Coord. Chem. Rev.* **2006**, *250*, 1332–1350.
- (16) Ouyang, L. Z.; Rulis, P.; Ching, W. Y.; Nardin, G.; Randaccio, L. *Inorg. Chem.* **2004**, *43*, 1235–1241.
- (17) Brown, K. L.; Zou, X.; Marques, H. M. *J. Mol. Struct.: THEOCHEM* **1998**, *453*, 209–224.
- (18) Marques, H. M.; Zou, X.; Brown, K. L. *J. Mol. Struct.* **2000**, *520*, 75–95.
- (19) Marques, H. M.; Brown, K. L. *Coord. Chem. Rev.* **2002**, *225*, 123–158.
- (20) Kobylanskii, I. J.; Widner, F. J.; Krautler, B.; Chen, P. *J. Am. Chem. Soc.* **2013**, *135*, 13648–51.
- (21) Grimme, S.; Antony, J.; Ehrlich, S.; Krieg, H. *J. Chem. Phys.* **2010**, *132*, 154104.
- (22) Grimme, S.; Ehrlich, S.; Goerigk, L. *J. Comput. Chem.* **2011**, *32*, 1456–1465.
- (23) Weymuth, T.; Couzijn, E. P. A.; Chen, P.; Reiher, M. *J. Chem. Theory Comput.* **2014**, *10*, 3092–3103.
- (24) Grimme, S.; Djukic, J.-P. *Inorg. Chem.* **2010**, *49*, 2911–2919.
- (25) Grimme, S.; Djukic, J.-P. *Inorg. Chem.* **2011**, *50*, 2619–2628.
- (26) Ryde, U.; Mata, R. A.; Grimme, S. *Dalton Trans.* **2011**, *40*, 11176–11183.
- (27) Grimme, S. *ChemPhysChem* **2012**, *13*, 1407–1409.
- (28) Steinmetz, M.; Grimme, S. *ChemistryOpen* **2013**, *2*, 115–124.
- (29) Hansen, A.; Bannwarth, C.; Grimme, S.; Petrović, P.; Werlé, C.; Djukic, J.-P. *ChemistryOpen* **2014**, *3*, 177–189.
- (30) Petrovic, P. V.; Grimme, S.; Zaric, S. D.; Pfeffer, M.; Djukic, J.-P. *Phys. Chem. Chem. Phys.* **2014**, *16*, 14688–14698.
- (31) Siegbahn, P. E. M.; Blomberg, M. R. A.; Chen, S. L. *J. Chem. Theory Comput.* **2010**, *6*, 2040–2044.
- (32) Kozłowski, P. M.; Kumar, M.; Piecuch, P.; Li, W.; Bauman, N. P.; Hansen, J. A.; Lodowski, P.; Jaworska, M. *J. Chem. Theory Comput.* **2012**, *8*, 1870–1894.
- (33) Kesharwani, M. K.; Martin, J. M. L. *Theor. Chem. Acc.* **2014**, *133*, 1452.
- (34) Zhang, W.; Truhlar, D. G.; Tang, M. *J. Chem. Theory Comput.* **2013**, *9*, 3965–3977.
- (35) Kepp, K. P. *J. Phys. Chem. A* **2014**, *118*, 7104–7117.

- (36) Andruniow, T.; Zgierski, M. Z.; Kozłowski, P. M. *J. Phys. Chem. B* **2000**, *104*, 10921–10927.
- (37) Andruniow, T.; Zgierski, M. Z.; Kozłowski, P. M. *J. Am. Chem. Soc.* **2001**, *123*, 2679–2680.
- (38) Dolker, N.; Morreale, A.; Maseras, F. J. *Biol. Inorg. Chem.* **2005**, *10*, 509–517.
- (39) Kuta, J.; Patchkovskii, S.; Zgierski, M. Z.; Kozłowski, P. M. *J. Comput. Chem.* **2006**, *27*, 1429–1437.
- (40) Jensen, K. P.; Ryde, U. *Coord. Chem. Rev.* **2009**, *253*, 769–778.
- (41) Hirao, H. *J. Phys. Chem. A* **2011**, *115*, 9308–9313.
- (42) Bucher, D.; Sandala, G. M.; Durbeej, B.; Radom, L.; Smith, D. M. *J. Am. Chem. Soc.* **2012**, *134*, 1591–1599.
- (43) Rodgers, M. T.; Ervin, K. M.; Armentrout, P. B. *J. Chem. Phys.* **1997**, *106*, 4499–4508.
- (44) Narancic, S.; Bach, A.; Chen, P. J. *J. Phys. Chem. A* **2007**, *111*, 7006–7013.
- (45) Armentrout, P. B.; Ervin, K. M.; Rodgers, M. T. *J. Phys. Chem. A* **2008**, *112*, 10071–10085.
- (46) Armentrout, P. B. *J. Am. Chem. Soc.* **2013**, *24*, 173–185.
- (47) Vydrov, O. A.; Van Voorhis, T. J. *Chem. Phys.* **2010**, *133*, 244103.
- (48) Hujo, W.; Grimme, S. *J. Chem. Theory Comput.* **2011**, *7*, 3866–3871.
- (49) Becke, A. D. *Phys. Rev. A* **1988**, *38*, 3098–3100.
- (50) Lee, C.; Yang, W.; Parr, R. G. *Phys. Rev. B* **1988**, *37*, 785–789.
- (51) Tao, J. M.; Perdew, J. P.; Staroverov, V. N.; Scuseria, G. E. *Phys. Rev. Lett.* **2003**, *91*, 146401.
- (52) Zhao, Y.; Truhlar, D. G. *J. Phys. Chem. A* **2005**, *109*, 5656–5667.
- (53) Zhao, Y.; Truhlar, D. *Theor. Chem. Acc.* **2008**, *120*, 215–241.
- (54) Hansen, A.; Liakos, D. G.; Neese, F. J. *Chem. Phys.* **2011**, *135*, 214102.
- (55) Klamt, A. *J. Phys. Chem.* **1995**, *99*, 2224–2235.
- (56) Klamt, A. *WIREs: Comput. Mol. Sci.* **2011**, *1*, 699–709.
- (57) Ahlrichs, R.; Bär, M.; Häser, M.; Horn, H.; Kölmel, C. *Chem. Phys. Lett.* **1989**, *162*, 165–169.
- (58) Ahlrichs, R.; Armbruster, M. K.; Bachorz, R. A.; Bär, M.; Baron, H.-P.; Bauernschmitt, R.; Bischoff, F. A.; Böcker, S.; Crawford, N.; Deglmann, P.; Sala, F. D.; Diedenhofen, M.; Ehrig, M.; Eichkorn, K.; Elliott, S.; Furche, F.; Glöß, A.; Haase, F.; Häser, M.; Hättig, C.; Hellweg, A.; Höfener, S.; Horn, H.; Huber, C.; Huniar, U.; Kattannek, M.; Klopper, W.; Köhn, A.; Kölmel, C.; Kollwitz, M.; May, K.; Nava, P.; Ochsenfeld, C.; Öhm, H.; Pabst, M.; Patzelt, H.; Rappoport, D.; Rubner, O.; Schäfer, A.; Schneider, U.; Sierka, M.; Tew, D. P.; Treutler, O.; Unterreiner, B.; von Arnim, M.; Weigend, F.; Weis, P.; Weiss, H.; Winter, N. *TURBOMOLE*; Version 6.4; TURBOMOLE GmbH: 2012.
- (59) Schäfer, A.; Horn, H.; Ahlrichs, R. *J. Chem. Phys.* **1992**, *97*, 2571–77.
- (60) Weigend, F. *Phys. Chem. Chem. Phys.* **2006**, *8*, 1057–1065.
- (61) Klamt, A.; Schuurmann, G. *J. Chem. Soc., Perkin Trans. 2* **1993**, 799–805.
- (62) Eichkorn, K.; Weigend, F.; Treutler, O.; Ahlrichs, R. *Theor. Chem. Acc.* **1997**, *97*, 119.
- (63) Deglmann, P.; May, K.; Furche, F.; Ahlrichs, R. *Chem. Phys. Lett.* **2004**, *384*, 103.
- (64) Grimme, S. *Chem. - Eur. J.* **2012**, *18*, 9955–9964.
- (65) Schäfer, A.; Huber, C.; Ahlrichs, R. *J. Chem. Phys.* **1994**, *100*, 5829–5835.
- (66) Weigend, F.; Häser, M.; Patzelt, H.; Ahlrichs, R. *Chem. Phys. Lett.* **1998**, *294*, 143–152.
- (67) Weigend, F.; Ahlrichs, R. *Phys. Chem. Chem. Phys.* **2005**, *7*, 3297–3305.
- (68) Eckert, F.; Klamt, A. *COSMOtherm*; Version C3.0, Release 12.01; COSMOlogic GmbH & Co. KG: Leverkusen, Germany, 2013.
- (69) Vosko, S. H.; Wilk, L.; Nusair, M. *Can. J. Phys.* **1980**, *58*, 1200–1211.
- (70) Perdew, J. P. *Phys. Rev. B* **1986**, *33*, 8822–8824.
- (71) Weigend, F.; Furche, F.; Ahlrichs, R. *J. Chem. Phys.* **2003**, *119*, 12753–12762.
- (72) Neese, F. *WIREs: Comput. Mol. Sci.* **2012**, *2*, 73–78.
- (73) Neese, F. *ORCA - an ab initio, density functional and semiempirical program package*; Version 3.0 (Rev. 1); MPI für Chemische Energiekonversion: Mülheim a. d. Ruhr (Germany), 2014.
- (74) Schaefer, A.; Huber, C.; Ahlrichs, R. *J. Chem. Phys.* **1994**, *100*, 5829–5835.
- (75) Halkier, A.; Helgaker, T.; Jørgensen, P.; Klopper, W.; Olsen, J. *Chem. Phys. Lett.* **1999**, *302*, 437–446.
- (76) Halkier, A.; Helgaker, T.; Jørgensen, P.; Klopper, W.; Koch, H.; Olsen, J.; Wilson, A. K. *Chem. Phys. Lett.* **1998**, *286*, 243–252.
- (77) Neese, F. *J. Am. Chem. Soc.* **2006**, *128*, 10213–10222.
- (78) Csaszar, A. G.; Allen, W. D.; Schaefer, H. F. J. *Chem. Phys.* **1998**, *108*, 9751–9764.
- (79) Hobza, P.; Sponer, J. *J. Am. Chem. Soc.* **2002**, *124*, 11802–11808.
- (80) Marshall, M. S.; Burns, L. A.; Sherrill, C. D. *J. Chem. Phys.* **2011**, *135*.
- (81) Rovira, C.; Kozłowski, P. M. *J. Phys. Chem. B* **2007**, *111*, 3251–3257.
- (82) Blanksby, S. J.; Ellison, G. B. *Acc. Chem. Res.* **2003**, *36*, 255–263.
- (83) Hay, B. P.; Finke, R. G. *J. Am. Chem. Soc.* **1987**, *109*, 8012–8018.
- (84) Luo, L. B.; Li, G.; Chen, H. L.; Fu, S. W.; Zhang, S. Y. *J. Chem. Soc., Dalton Trans.* **1998**, 2103–2107.
- (85) Ehrlich, S.; Moellmann, J.; Reckien, W.; Bredow, T.; Grimme, S. *ChemPhysChem* **2011**, *12*, 3414–3420.